2023 45th Annual International Conference of the IEEE Engineering in Medicine & Biology Conference (EMBC)

Proceedings

2023 45th Annual International Conference of the IEEE Engineering in Medicine & Biology Society (EMBC) | 979-8-3503-2447-1/23/$31.00 ©2023 IEEE | DOI: 10.1109/EMBC40787.2023.10340653

Sydney, Australia
24 - 27 July 2023

IEEE

IEEE eCP
eXpress Conference Publishing

IEEE Catalog Number: CFP23EMB-ART
ISBN: 979-8-3503-2447-1
Online ISSN: 2694-0604

2023 45th Annual International Conference of the IEEE Engineering in Medicine & Biology Society (EMBC) | 979-8-3503-2447-1/23/$31.00 ©2023 IEEE | DOI: 10.1109/EMBC40787.2023.10340069

2023 45th Annual International Conference of the IEEE Engineering in Medicine & Biology Conference (EMBC)

IEEE Catalog Number: CFP23EMB-ART

ISBN: 979-8-3503-2447-1

Online ISSN: 2694-0604

Printed copies of this publication are available from:

Curran Associates, Inc
57 Morehouse Lane
Red Hook, NY 12571 USA
Phone: (845) 758-0400
Fax: (845) 758-2633
E-mail: curran@proceedings.com

2023 45th Annual International Conference of the IEEE Engineering in Medicine & Biology Society (EMBC) | 979-8-3503-2447-1/23/$31.00 ©2023 IEEE | DOI: 10.1109/EMBC40787.2023.10340275

Analysis of Error Potentials generated by a lower limb exoskeleton feedback in a BMI for gait control*

P. Soriano-Segura, L. Ferrero, *Student Member,* M. Ortiz, *Member, IEEE*, E. Iáñez, *Member, IEEE*, and J. M. Azorín, *Senior Member, IEEE*

***Abstract* —Brain-machine interfaces (BMIs) based on motor imagery (MI) for controlling lower-limb exoskeletons during the gait have been gaining importance in the rehabilitation field. However, these MI-BMI are not as precise as they should. The detection of error related potentials (ErrP) as a self-tune parameter to prevent wrong commands could be an interesting approach to improve their performance. For this reason, in this investigation ErrP elicited by the movement of a lower-limb exoskeleton against subject's will is analyzed in the time, frequency and time-frequency domain and compared with the cases where the exoskeleton is correctly commanded by motor imagery (MI). The results of the ErrP study indicate that there is statistical significative evidence of a difference between the signals in the erroneous events and the success events. Thus, ErrP could be used to increase the accuracy of BMIs which commands exoskeletons.**

***Clinical Relevance*— This investigation has the purpose of improving brain-machine interfaces (BMIs) based on motor imagery (MI) by means of the detection of error potentials. This could promote the adoption of robotic exoskeletons commanded by BMIs in rehabilitation therapies.**

I. Introduction

Brain-Machine Interfaces (BMIs) involve the utilization of signals generated by the brain to control an external device, such as an exoskeleton [1][2]. The use of BMIs and exoskeletons in the rehabilitation of patients with motor injuries is a promising technology as it allows the patient to take control of their rehabilitation, providing a more effective and efficient recovery process [3][4]. A BMI based on Motor Imagery (MI) paradigm with an exoskeleton is one of the most common choices for the rehabilitation of motor abilities in patients, because of the realism and implication of the subjects in the task. However, the robustness of this type of BMI is not as high as it should be for a correct performance, particularly in the rehabilitation of lower limbs [5][6]. One of the main reasons is the fact that legs are represented in the internal region of the brain between both hemispheres. Hence, the signals of the gait imagination are weaker and more difficult to detect.

Over the past years, some investigations have combined the motor imagery commands with error related potentials (ErrP) with the intention of solving this problem and improving the MI-BMI performance. These error potentials are generated as a response when the subject detects that the device is not working as it was expected. For instance, an ErrP would be elicited when the patient tries starting the gait by MI, but the exoskeleton remains standing as the BMI is not detecting the MI. In this case, if the ErrP is detected, the incorrect command decoded by the BMI, i.e., the relax state, would be self-tuned, generating the right command for starting the gait. Accordingly, the BMI performance would be enhanced [7].

The ErrP has been studied in the literature throughout the years by many researchers. It has been proved that these potentials are stable in time and amplitude [8][9][10]. However, the subjects could get used to the error situation if it is repeated many times in a short period of time, complicating its detection [10][11]. It has been found that there are differences between the ErrP in monitoring and control tasks, which leaded [9] to brand the interaction ErrP for control BMI. The interaction ErrP is characterized, in an approximate window of 450ms after the feedback, by four peaks: a small positive peak (P1) followed by a pronounced negative peak (N1), then the potential increments into a large positive peak (P2) and the potential decrements again to generate the final negative peak (N2). Many investigations have found the ErrP produced by an error in decoding MI commands [7][9][11][12][13]. In addition, [12] indicates that the MI time or Inter-Stimulus Interval has influence in the appearance of the ErrP. The research shows that the higher the time of imagining is, the better ErrP is detected, but it takes more time to show after the feedback. Furthermore, the ErrP shape and detection precision may vary depending on the type of feedback the subject receives. [14] exposes that the combination of visual and tactile feedback has higher precision than visual feedback by itself, and also confirms that ErrP takes longer to appear after the feedback. [13] compares visual feedback with proprioceptive feedback provided by the movement of an exoskeleton, finding out there are no traces of the ErrP for the proprioceptive feedback.

In the present work, the ErrP elicited by the proprioceptive feedback of an exoskeleton using a MI-BMI to start the gait task is analyzed. The EEG and exoskeleton data generated following the experimental protocol in [5] is used to compare

*Research supported by: Valencian Graduate School and Research Network of Artificial Intelligence (ValgrAI), Generalitat Valenciana and European Union; grant PID2021-124111OB-C31, funded by MCIN/AEI/10.13039/501100011033 and by ERDF A way of making Europe; and Ministry of Science, Innovation and Universities through the Aid for the Training of University Teachers FPU19/03165.

P. Soriano-Segura, L. Ferrero, M. Ortiz, E. Iáñez and J.M. Azorín are researchers in the Brain- Machine Interface System Lab at Miguel Hernández University of Elche, Miguel Hernández University of Elche, Elche, Spain (e-mail: p.soriano@umh.es, lferrero@umh.es, mortiz@umh.es, eianez@umh.es, jm.azorin@umh.es).

M. Ortiz, E. Iáñez and J.M. Azorín are researchers in Instituto de Investigación en Ingeniería de Elche-I3E, Miguel Hernández University of Elche, 03202 Elche, Spain.

J.M. Azorín is associate researcher at the Valencian Graduate School and Research Network of Artificial Intelligence – valgrAI, Spain.

the following events: TP events when the exoskeleton moves due to the subject's intention to start walking, and FP events when the exoskeleton moves against subject's will.

II. Material and Methods

A. Equipment

EEG signals were recorded using the Starstim R32 device (Neuroelectrics, Spain) at a sampling rate of 500 Hz. The cap is composed of 32 non-invasive wet electrodes. 27 channels following the 10-10 distribution of the international system were used to register the EEG signals: F3, FZ, FC1, FCZ, C1, CZ, CP1, CPZ, FC5, FC3, C5, C3, CP5, CP3, P3, PZ, F4, FC2, FC4, FC6, C2, C4, CP2, CP4, C6, CP6, P4. The reference and ground electrodes are located on the right ear lobe.

Subjects' movements are supported by H3 exoskeleton (Technaid, Madrid, Spain), whose control commands are received through Bluetooth. The subjects also use crutches to maintain the stability during the gait.

B. Experimental protocol

The original protocol that was used to collect the data consisted in a MI-BMI that controlled the start and stop of a lower-limb exoskeleton [5]. During the trials, different tasks were performed by the subject, who received the order by voice message. Each session was divided into two: a training stage and a test stage. The training stage was an open-loop control where the subject executed three different mental tasks within the same trial: relax, motor imagery of the gait and a regressive mathematical subtraction with three digits numbers. Each subject performed 23 trials during this stage for training the MI classifier. During the test stage, the exoskeleton was in a closed-loop control. The subject began relaxed and then, he/she performed a motor imagery of the gait with the purpose of activating the exoskeleton to start walking and keep it on till a new relax phase for stopping was required. Each subject performed 10 trials in the closed-loop stage.

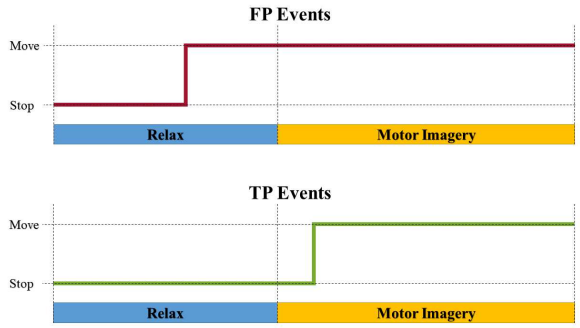

Figure 1. The two events that are analyzed in the study are shown. In FP Events (up), exoskeleton wrongly activates within relax window. In TP Events (down), exoskeleton activates successfully for the first time within motor imagery window by means of a subject imagined command.

In this study, only the test trials in closed loop are considered for the ErrP analysis. In the study, two types of events that happened within the trials are analyzed (Figure 1): The error events, that occur when the subject activates wrongly the exoskeleton during the initial relax time (false positives FP during the first relax), and the success events, when the subject activates the exoskeleton for the first time within the motor imagery window (first true positives TP). Each subject performed 5 sessions of the experiment with 10 trials in each session. Notice that not all the trials gave the same information about the studied events, as it depends on the actual FPs and TPs detected, obtaining a different number of class events per trial.

C. EEG Signal Processing

The data acquired during the sessions were first preprocessed in order to find the event windows and conditions for studying the ErrP.

Firstly, the EEG signals in the 27 channels were filtered by a state variable band-pass filter between 1 and 7 Hz. The main intention of extracting these frequency bands was filtering the bands where the signals of error events are highly discriminable from correct events signals, as it is described in [15]. Then, a Laplacian spatial filter was applied to improve the spatial information.

Afterwards, the sample where the exoskeleton activates is used to define the analysis window. An activation point within the relax window is labeled as error event (FP) and withing the motor imagery window as success event (TP). Therefore, trials are cropped in epochs of 0.5 seconds before the event and 1.5 seconds after the event. As a result of splitting all the trials in event periods, the dataset is divided in 80 FP and 112 TP. The imbalance of the dataset is a consequence of not all the trials containing both events.

D. ErrP Analysis

The processed EEG signals are analyzed in the time domain, frequency domain and time-frequency domain at electrode FCz, which is the nearest electrode to ACC (anterior cingulate cortex) where the ErrP is generated [16]. The aim is finding differences and similarities between FP and TP events.

In the time domain analysis, amplitude differences between FP and TP events are examined. FCz data are averaged for all subjects and for each subject separately. Looking at each subject's ErrP separately is interesting because the global average ErrP signal can be completely altered by just a single trial with higher amplitude peaks than the rest. In the frequency domain analysis, the FFT Power Spectrum is obtained as the average of squared absolute values of the FFT output. Finally, in the time-frequency analysis, the frequency power distribution is estimated again, but now in each interval of time and frequency by using the Wavelet transform (Morlet wavelet as mother). For the representation, scalp topographic maps are computed for the time samples where signal in electrode FCz presents the ErrP main peaks (N1, P1, N2, P2) to visualize the signal distribution in the different electrodes and brain regions.

Additionally, a statistical rank-sum Wilcoxon test with a confidence of 5% is performed to compare the global average signal in FP with the one in TP events. Moreover, the statistic test is carried out comparing the FP and TP signals of each subject and, also comparing the ErrP signals of between subjects. Thus, it is possible to explore variances in the ErrP signals of the participants.

E. *Subjects*

Five subjects participated in the study with ages between 24 and 27 years old (25.6±1.5). None of the subjects reported any diseases and was not under medical treatment. All the subjects gave a written informed consent to participate according to Helsinki declaration. The study was approved by the Responsible Research Office of Miguel Hernández University of Elche (Spain) (DIS.JAP.03.18).

III. Results

Figure 2 summarizes the results of the ErrP analysis in the time, frequency, and time-frequency domain. Figure 2.A exposes the global average ErrP signal of all subjects for FP (red) and TP (green) classes. FP class average presents a prominent negative peak (N1) at 240ms after the exoskeleton starts, followed by a positive peak (P1) at 370ms, another negative peak (N2) at 630ms followed by another positive peak (P2) at 720ms. This error signal seems quite different from the success signal, which stays constant after the feedback. The statistical test of Wilcoxon confirms that there is evidence of a significant difference between the ErrP in FP and TP classes with a confidence of $p < 5\%$. Moreover, the difference between the classes is more obvious in the scalp topographical maps (Figure 2.C). In these graphics, FP class presents negative (N1) and positive (P1) potentials in the frontocentral regions after the feedback, while the TP class remains stable until N2, where both classes look quite similar with a potential decreasing in the central area. In the last peak (P2) both classes are completely different again, while FP class has a potential increase in the ACC region, TP class presents a diminution of the potential at this location.

Parallelly, the comparative between the ErrP of each subject (Figure 2.B) indicates that subjects S1 and S5 are similar in shape and, they are the main contributors to N1 in the global average ErrP signal. Whereas the ErrP of subject S2 presents a similar shape with the previous subjects, but with a certain delay. However, subjects S3 and S4 ErrP differs not only in time, but also in the shape with the rest. The ErrP of these two participants is the cause of the second negative deflection N2 at 630ms after the exoskeleton movement in the average signal of Figure 2.A. The statistical test between subjects indicates that subjects S1, S2 and S5 are statistically equal, but there is also evidence that they are significantly different from subjects S3 and S4 with a confidence of $p < 5\%$. Furthermore, another statistical test confirmed that subjects S3 and S4 are not statistically different.

Conversely, in the frequency and time-frequency analysis (Figure 2.D) the dissimilarity between FP and TP classes is not as clear as it is in the time domain. The power distribution is concentrated in the first second right after the beginning of the gait throughout the frequency axis. However, the power is more pronounced at 500-600ms between 3-5 Hz for FP class. Another difference found is the fact that the higher power spectrum values (orange and red) are wider for FP class, due to the time differences between both classes. Precisely, TP class values increase around 400ms after the feedback, instead of earlier in time like FP class does around 200ms.

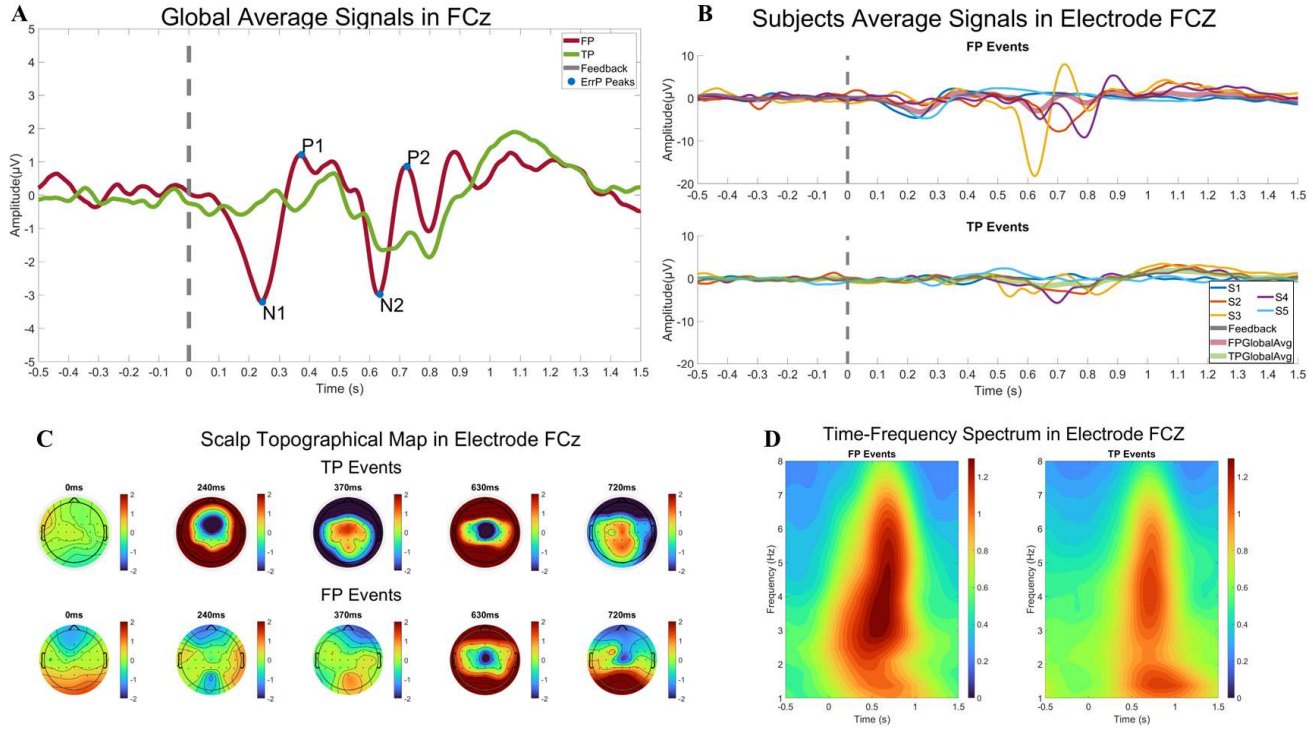

Figure 2. Compares signals of electrode FCz in FP and TP events. A is a comparative between the global average signal of electrode FCz in FP and TP events in time domain. B shows the signals average of each subject of electrode FCz in FP (top) and TP (down) events. C is the topographical representation of the electrodes for FP and TP events at the peak points in the ErrP signal. D represents frequency power distribution in time-frequency domain for FP (left) and TP (right) events.

IV. Discussion

In the present research, the appearance of ErrP during the performance of a MI-BMI to control the gait with an exoskeleton is studied. Particularly, the ErrP should only emerge in those cases the exoskeleton moves when it should remain static. The peculiarity of this investigation is the fact that the subjects are on their feet and moving during the trials, whereas in general this potential has been detected during relax tasks in the literature [7][8][9][10][11][12][14]. This scenario supposes a relevant challenge because of the number of mixed potentials at the time. For this reason, the EEG signals are filtered in low frequencies (delta and theta bands) [15], instead of including alfa and beta bands, with the aim of avoiding as movement noise as it is possible and being able to differentiate TP and FP classes more clearly. Another characteristic of this research is the proprioceptive feedback carried out by the exoskeleton moving the legs that is used to generate the ErrP. There is only one similar case in the literature using an upper-limb exoskeleton to elicit ErrP and it did not find any evidence of the presence of the desired potential [13]. Nevertheless, the present study has shown the presence of it.

A significative difference between FP and TP classes have been evidenced statistically. However, these dissimilarities are more perceptible on the time domain rather than the frequency domain. In the time domain, the shape of the ErrP is composed of a pronounced negative peak (N1) at 240ms after the feedback, followed by a small positive peak (P1) at 370ms, another negative peak (N2) at 630ms once again followed by a small positive peak (P2) at 720ms. This global average signal looks like the grand average ErrP generated because of visuo-tactile feedback that was reported in [14]. Nevertheless, this signal has similarity in time, but not in shape at all, with the interaction ErrP already described in [9], probably because of the lag in the ErrP occurrence between subjects. Subjects S1 and S5 ErrP is shown around 200ms after the feedback, while subjects S2, S3 and S4 ErrP signals take more time to show. Statistical tests have demonstrated that subjects S1, S2 and S5 ErrPs are similar between them and different of subjects S3 and S4 ErrP. The ErrP of these two subjects is also similar to them. To sum up, although the significative difference between FP and TP classes is such a promising result, the number of samples analyzed is not large enough for generalization due to the variance of ErrP across the subjects.

Future research will study the use of the ErrP to design a self-tuned BMI to correct the apparition of FPs, avoiding the generation of wrong commands. This would mean that the ErrP would not be generated by the feedback of the exoskeleton movement but with a warning, as the exoskeleton activation has to be prevented by the system.

References

[1] D. J. McFarland and J. R. Wolpaw, "Brain-computer interfaces for communication and control," Commun ACM, vol. 54, no. 5, pp. 60–66, May 2011, doi: 10.1145/1941487.1941506.

[2] R. P. N. Rao, Brain-Computer Interfacing. Cambridge University Press, 2013. doi: 10.1017/CBO9781139032803.

[3] K. K. Ang and C. Guan, "Brain-Computer Interface in Stroke Rehabilitation," Journal of Computing Science and Engineering, vol. 7, no. 2, pp. 139–146, Jun. 2013, doi: 10.5626/JCSE.2013.7.2.139.

[4] A. Caria et al., "Chronic stroke recovery after combined BCI training and physiotherapy: A case report," Psychophysiology, vol. 48, no. 4, pp. 578–582, Apr. 2011, doi: 10.1111/j.1469-8986.2010.01117.x.

[5] L. Ferrero, V. Quiles, M. Ortiz, E. Iáñez, and J. M. Azorín, "A BMI Based on Motor Imagery and Attention for Commanding a Lower-Limb Robotic Exoskeleton: A Case Study," Applied Sciences, vol. 11, no. 9, p. 4106, Apr. 2021, doi: 10.3390/app11094106.

[6] L. Ferrero, E. Ianez, V. Quiles, J. M. Azorin, and M. Ortiz, "Adapting EEG based MI-BMI depending on alertness level for controlling a lower-limb exoskeleton," in 2022 IEEE International Conference on Metrology for Extended Reality, Artificial Intelligence and Neural Engineering (MetroXRAINE), Oct. 2022, pp. 399–403. doi: 10.1109/MetroXRAINE54828.2022.9967639.

[7] Y. Zhang, W. Chen, C.-L. Lin, J. Chu, and F. Meng, "Research on Command Confirmation Unit Based on Motor Imagery EEG Signal Decoding Feedback in Brain-Computer Interface," in 2018 15th International Conference on Control, Automation, Robotics and Vision (ICARCV), Nov. 2018, pp. 1923–1928. doi: 10.1109/ICARCV.2018.8581088.

[8] P. W. Ferrez and J. del R. Millan, "Error-Related EEG Potentials Generated During Simulated Brain–Computer Interaction," IEEE Trans Biomed Eng, vol. 55, no. 3, pp. 923–929, Mar. 2008, doi: 10.1109/TBME.2007.908083.

[9] P. W. Ferrez and J. del R. Millan, "Simultaneous Real-Time Detection of Motor Imagery and Error-Related Potentials for Improved BCI Accuracy," Proceedings of the 4th International Brain-Computer Interface Workshop and Training Course, pp. 197–202, 2008, [Online]. Available: https://www.researchgate.net/publication/41386722

[10] R. Chavarriaga and J. del R. Millan, "Learning From EEG Error-Related Potentials in Noninvasive Brain-Computer Interfaces," IEEE Transactions on Neural Systems and Rehabilitation Engineering, vol. 18, no. 4, pp. 381–388, Aug. 2010, doi: 10.1109/TNSRE.2010.2053387.

[11] L. Schiatti, G. Barresi, J. Tessadori, L. C. King, and L. S. Mattos, "The Effect of Vibrotactile Feedback on ErrP-based Adaptive Classification of Motor Imagery," in 2019 41st Annual International Conference of the IEEE Engineering in Medicine and Biology Society (EMBC), Jul. 2019, pp. 6750–6753. doi: 10.1109/EMBC.2019.8857192.

[12] B. Ahkami and F. Ghassemi, "Adding Tactile Feedback and Changing ISI to Improve BCI Systems' Robustness: An Error-Related Potential Study," Brain Topogr, vol. 34, no. 4, pp. 467–477, Jul. 2021, doi: 10.1007/s10548-021-00840-6.

[13] S. M. Meyer, A. Rao Mangalore, S. K. Ehrlich, N. Berberich, J. Nassour, and G. Cheng, "A Comparative Pilot Study on ErrPs for Different Usage Conditions of an Exoskeleton with a Mobile EEG Device," in 2021 43rd Annual International Conference of the IEEE Engineering in Medicine & Biology Society (EMBC), Nov. 2021, pp. 6203–6206. doi: 10.1109/EMBC46164.2021.9630465.

[14] J. Tessadori, L. Schiatti, G. Barresi, and L. S. Mattos, "Does tactile feedback enhance single-trial detection of error-related eeg potentials?" in 2017 IEEE International Conference on Systems, Man, and Cybernetics (SMC), Oct. 2017, pp. 1417–1422. doi: 10.1109/SMC.2017.8122812.

[15] J. Omedes, I. Iturrate, and L. Montesano, "Brain connectivity in continuous error tasks," in 2014 36th Annual International Conference of the IEEE Engineering in Medicine and Biology Society, Aug. 2014, pp. 3997–4000. doi: 10.1109/EMBC.2014.6944500.

[16] D. H. Mathalon, S. L. Whitfield, and J. M. Ford, "Anatomy of an error: ERP and fMRI," Biol Psychol, vol. 64, no. 1–2, pp. 119–141, Oct. 2003, doi: 10.1016/S0301-0511(03)00105-4.